ELSEVIER

Contents lists available at ScienceDirect

Journal of Alloys and Compounds

journal homepage: http://www.elsevier.com/locate/jalcom



Catalytic decoloration of commercial azo dyes by copper-carbon composites derived from metal organic frameworks



Zubair Hasan ^a, Dong-Wan Cho ^a, Gazi Jahirul Islam ^b, Hocheol Song ^{a,*}

- ^a Department of Environment and Energy, Sejong University, Seoul, 143-747, South Korea
- ^b Department of Chemistry, University of Barisal, Bangladesh

ARTICLE INFO

Article history: Received 10 June 2016 Received in revised form 26 July 2016 Accepted 4 August 2016 Available online 7 August 2016

Keywords:
Metal-organic framework
Composites
Non-noble metal catalyst
Decoloration
Methylene blue
Rhodamine B

ABSTRACT

Porous copper-carbon composites were synthesized via one-step heat treatment of copper-based metal organic frameworks (MOFs), MOF-199. The prepared composites, Cu-CC-550 and Cu-CC-650, were applied as catalysts for catalytic decoloration of two commercial azo dyes, methylene blue (MB) and rhodamine B (RB) in the presence of NaBH4. The composites were characterized by a series of spectroscopic instruments and a surface analyzer. The characterization confirmed the presence of Cu_2O and Cu in the amorphous carbon network with high porosity. The composites were very active in decolorizing MB, RB, and their mixture. In particular, Cu-CC-550exhibited a great reusability to complete five consecutive MB reduction cycles with a minimal loss of catalytic capability and structural integrity. The prepared Cu-CC composite can be considered as a promising material for catalytic decoloration of dyes as well as a potential alternative to replace noble metal-based catalysts.

© 2016 Elsevier B.V. All rights reserved.

1. Introduction

During the last few decades, the consumption of synthetic dyes in different industries including paper, plastics, textile, leather, and food processing has significantly increased, and wastewater effluents from those industries have created a great public concern about dye pollution in the receiving water bodies [1]. In last decade, over 7×10^5 tons of around 100,000 different types of commercial dyes were produced and roughly 100 tons of dyes were discharged into water streams [2,3]. Many of these colored contaminants are toxic, carcinogenic and non-biodegradable [4]. Overexposure to dyes can cause skin irritation, respiratory problems, kidney dysfunction, damage of reproductive system, liver or brain, and impairment of central nervous system in humans [5]. In addition, dyes consume dissolved oxygen, and interfere with photosynthetic activity of aquatic plants [4].

The conventional microbial mediated wastewater treatments often suffer from low efficiencies in dyes removal because of poor biodegradability of dyes and the deterrent effects of high salt concentration in dye-wastewaters [6]. As a consequence, a number of methods have been reported for dyes removal including

Corresponding author.

E-mail address: hcsong@sejong.ac.kr (H. Song).

coagulation/flocculation [7], adsorption [6], photo-catalysis [8], and oxidation processes [9]. Most of the existing methods are more or less effective in removal of dyes, however, some of them have encountered operational disadvantages. For example, a large amount of sludge is generated in coagulation/flocculation because of the use of various chemical reagents including polyelectrolytes and coagulants [10]. Fenton's reagent (H_2O_2/Fe^{2+}) or ozoneassisted advanced oxidation process can effectively remove dyes without sludge production, however, it suffers from high operating cost and short lifetime of oxidants [11]. The photocatalytic degradation of dyes under UV radiation needs long operating time and the use of UV radiation limits its large-scale application [12]. On the other hand, removal of dyes via adsorption has practical advantages due to its simple operation and good efficiencies, but it has problems associated with adsorbent disposal and post-contamination by used adsorbents [6]. For these reasons, research interests overdevelopment of new types of adsorbents, catalysts and other effective methods for dyes treatment still continue to grow.

Recently, NaBH₄-assisted catalytic reduction of dyes is gaining much attention because of its fast and simple operation procedure [6,13–19]. As catalysts, noble metal nanoparticles (e.g., Pd, Pt, Au, Ag, and Ru) on silica or carbon supports have been widely used for their high efficiencies [13–15]. However, the scarcity and high cost of noble metals impede wide and practical application of noble

metal catalysts [6,16]. As a consequence, substitution of noble metal based catalysts by non-noble metal based catalysts has become an important research topic in recent years.

As an effort to develop non-noble metal catalysts, several researchers have investigated the use of metal-organic frameworks (MOFs) as a base material [20–23]. MOFs materials have several advantageous properties such as high porosity, controllable pore size, and ability to impart specific functionalities or active species without altering the framework topology [24–26]. In preparation of catalysts, MOFs are used as a sacrificing template or platform while providing carbon sources such as farfural alcohol, phenolic resin, glycerol, and carbon tetrachloride [27]. Recently, direct calcination of MOFs (without any additional carbon source) has also been reported to prepare MOF-derived metal or metal oxide/carbon composites [21–23]. These metal/carbon composites showed promising performances as catalysts or absorbents [22,23,28].

In this study, Cu-carbon composites (Cu-CC) were prepared via simple calcination of a Cu-based MOF, MOF-199 (Cu linked by 1,3,5-benzinetricarboxylic acid [29]), under N₂ atmosphere, and the composites were used as catalysts for decoloration of two common industrial dyes, methylene blue (MB) and rhodamine B (RB) (Scheme 1). The prepared composites were characterized using various spectroscopic methods and a surface analyzer, and a series of batch reduction experiments were carried out to demonstrate the catalytic capability of the composites.

2. Experimental methods

2.1. Materials

All the chemicals and reagents were purchased from commercial vendors and used as received. 1,3,5-benzinetricarboxylic acid ($C_9H_6O_6$, H_3BTC , 98%), $RB(C_{28}H_{31}ClN_2O_3>95\%)$, and MB ($C_{16}H_{18}N_3SCl$) were obtained from Alfa Aeser, USA. Copper (II) nitrate hemihydrate (($Cu(NO_3)_2 \cdot 2.5H_2O$, >97%), sodium borohydride (NaBH₄, extra pure), methanol (CH_3OH , >99.5%), ethanol (C_2H_5OH , 99.9%), N,N-dimethylformamide (C_3H_7NO , >99.5%), hydrochloric acid (HCl, 35.5%) and nitric acid (HNO₃, 60%) were purchased from Daejung Chemical, South Korea.

2.2. Synthesis of MOF-199

MOF-199 was prepared according to the method of Hu et al. [30] with a minor modification. In brief, 1.0 g H₃BTC and 1.95 g

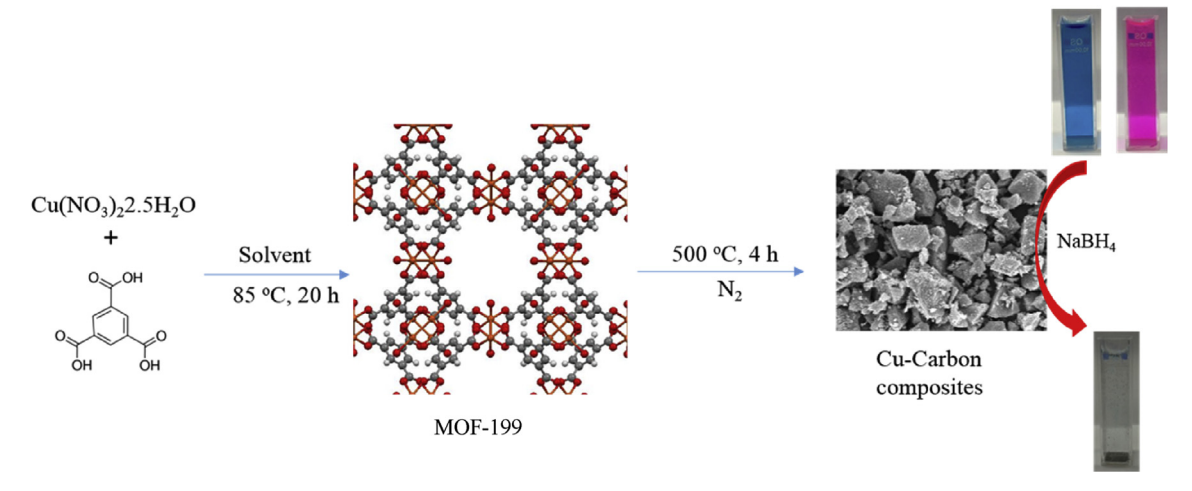
 $\text{Cu}(\text{NO}_3)_2 \cdot 2.5\text{H}_2\text{O}$ were dissolved in 51 mL solvent mixture (water: ethanol: N,N-dimethylformamide, 1:1:1 (v/v/v)), and the mixture was mixed for 10 min with magnetic stirring. The solution was taken into a Teflon lined autoclave vessel, sealed and placed in an oven (wiseven, Korea), and heated for 20 h at 85 °C. After the reaction, the solution was cooled down while allowing precipitation of blue solid products. The precipitates were collected by filtration, washed with ethanol several times to remove residual H_3 BTC, and dried for 12 h at 100 °C.

2.3. Synthesis of Cu-carbon composites

MOF-199 was taken in an alumina crucible, and placed in a tubular reactor for thermal treatment. A 610 mm long quartz tube with 25.4 mm outer diameter (Chemglass CGQ-0900T-13) was used as a tubular reactor. The reactor was heated at 550 °C or 650 °C for 4 h using a split-hinged furnace (AsOne, Japan). The heating rate was 5 °C min⁻¹ and an S-type thermocouple was used to monitor the temperature. The N₂ gas flow rate was fixed at 500 mL min⁻¹ using a Brooks mass flow controller (5850 series E), and a computer-aided control system by LabVIEW (National Instrument, USA) was employed to control the flow. After cooling to room temperature, the powder products were retrieved, washed several times with water and ethanol, dried at 100 °C overnight, and kept in a sealed vial before use. The products were designated as Cu-CC-550 or Cu-CC-650 depending on the heating temperature.

2.4. Characterization

X-ray powder diffraction (XRD) analysis was conducted with the Rigaku DMax-2500 diffractometer using CuK α radiation. The surface area and pore size of the prepared samples were obtained from nitrogen adsorption method using a BELSORP-mini II (MicrotracBEL, Japan). The samples were evacuated at 150 °C for 12 h before nitrogen adsorption at -196 °C. Raman spectra were taken using an inVia reflex Raman microscope (Renishaw, UK). The morphologies and composition of the samples were examined with a field emission scanning electron microscope (FE-SEM, JEOL-JSM7401F). Surface analysis of the samples was conducted using a theta probe angle-resolved X-ray photoelectron spectrometer (ARXPS) system equipped with the monochromatic Al K α line (1486.7 eV). A Gaussian (30%)-Lorentzian (70%) model (defined in CasaXPS as GL (70)) was employed to generate the curve-fitting spectra of the Cu 2p3/2, Cu 1p1/2, O 1s, and C1s in depth XPS



Scheme 1. Preparation of Cu-CC composite and its application in dye decoloration.

profile of Cu-CC-550.

2.5. Catalytic dye decoloration

The catalytic decoloration of MB and RB, and their mixture were carried out in a standard quartz cuvette with a 1 cm path length in the presence of an excess amount of NaBH₄ at room temperature, and the progress of the reduction was monitored using a UV-vis spectroscopy (Hach DR/4000, USA). For decoloration of MB, 1.5 mL MB solution (50 mg L^{-1}), 1.5 mL DI water and 1 mL of freshly prepared NaBH₄ solution (0.04–0.25 M) were taken in a quartz cuvette. For RB, the cuvette was filled with 2.2 mL RB solution $(50\ mg\ L^{-1}), 1.3\ mL\ DI$ water, and $0.8\ mL\ NaBH_4\ solution\ (0.2\ M).$ For the decoloration of MB and RB mixture, the cuvette was filled with 1.2 mL MB (50 mg L^{-1}), 1.2 mL RB (50 mg L^{-1}), 1 mL DI water, and $0.8~mL~NaBH_4~solution~(0.2~M).$ Subsequently (for all cases), $50~\mu L$ (10 mg/mL, sonicated for 30 min before application to attain well dispersion) aqueous dispersion of Cu-CC composite was added to the cuvette, and the solution was quickly introduced to UV-Vis measurements. The absorbance of the solution was measured at different intervals within the scanning range of 400-800 nm.

3. Results and discussion

3.1. Characterization of the composites

The results of XRD analyses of the MOFs precursors and the composites are presented in Fig. 1(a). The XRD patterns of synthesized MOFs showed a very close agreement to the simulated MOF-199, validating successful synthesis of desired precursors. Fig. 1(a) also demonstrated that the structure of MOF-199 was completely collapsed during heat treatment at 550 °C, and simultaneously, new diffraction peaks were also evolved. The XRD spectra (Fig. 1(a)) of Cu-CC-550 composites showed the characteristic peaks at 36.3° and 61.3°, attributable to the (1 1 1) and (2 2 0) crystal planes of cubic Cu₂O (JCDS 78-2076), respectively, whereas the other three peaks originated at 43.3°, 50.3° and 74.1° could be assigned to the (1 1 1), (2 0 0) and (2 2 0) planes of metallic copper (JCPDS No: 4-0836), respectively [31]. Cu-CC-650 also exhibited XRD spectra similar to Cu-CC-550.

Raman spectra of Cu-CC composites are presented in Fig. 1(b). Both spectra showed peaks at 1345 and 1583 cm⁻¹, characterized as D (defects and disorder) and G (graphite) band, respectively, which are characteristic Raman peaks of carbon composites [32]. These peaks indicate the presence of amorphous carbon phases, both in Cu-CC-550 and Cu-CC-650, as there was no evidence of crystalline

carbon phase in the XRD spectra. The nitrogen adsorption isotherms of the samples are presented in Fig. 2, and results are summarized in Table S1. The BET surface area and the pore volume of MOF-199 were found to be 1356 $\rm m^2~g^{-1}$ and 0.71 cm $^3~g^{-1}$, respectively. However, after heat treatment at 550 °C, the surface area and pore volume were significantly reduced to 239 $\rm m^2~g^{-1}$ and 0.31 cm $^3~g^{-1}$, respectively. After calcination at 650 °C, a small increase in surface area relative to at 550 °C was observed (Table S1).

XPS analysis of Cu-CC-550 presented in Fig. 3 shows the oxidation state of copper and carbon phases. In Cu 2p scan, the main peak at 932.8 eV could be attributed to Cu (Cu 0) and/or Cu₂O (Cu $^{1+}$), and the peak at 934.7 eV to Cu(OH)₂ (Cu $^{2+}$) [33]. Besides, there exist two more shake-up peaks at 941.2 eV and 944.0 eV, which could be ascribed to Cu(OH)₂ as it is often observed in atmosphere-exposed Cu₂O surfaces [33,34]. Collectively, the existence of Cu(OH)₂ phase on Cu-CC-550 was clearly observed in XPS, but its occurrence was not very significant since XRD did not show any evidence of Cu(OH)₂.

The curve fitting spectra of O1s showed two main peaks at 530.2 and 531.8 eV, as well as a small peak at 533.7 eV (Fig. 3(b)). The peak at 530.2 eV could be attributable toCu₂O and Cu-OH groups [35,36], whereas, those at 531.8 and 533.7 eV to C-OH and C=O on the surface of the carbon matrix, respectively [35,37]. Moreover, the absence of peaks below 530 eV excludes the presence of CuO in the composites [36]. The curve fitting spectra of C 1s indicated the presence of C-C (284.6 eV) as a dominating carbon phase along with

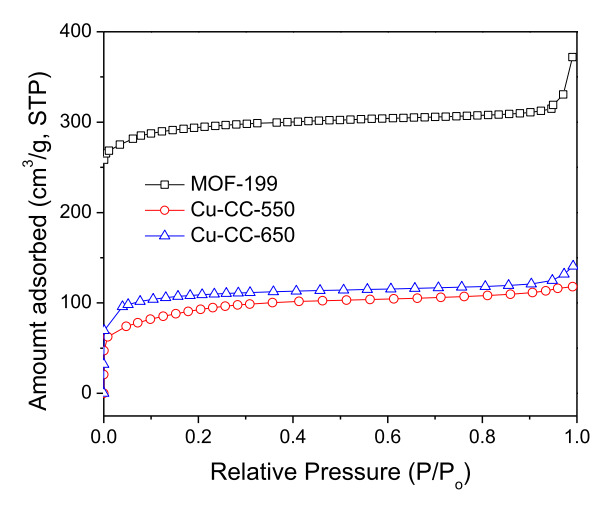


Fig. 2. N₂ adsorption isotherms of the prepared samples.

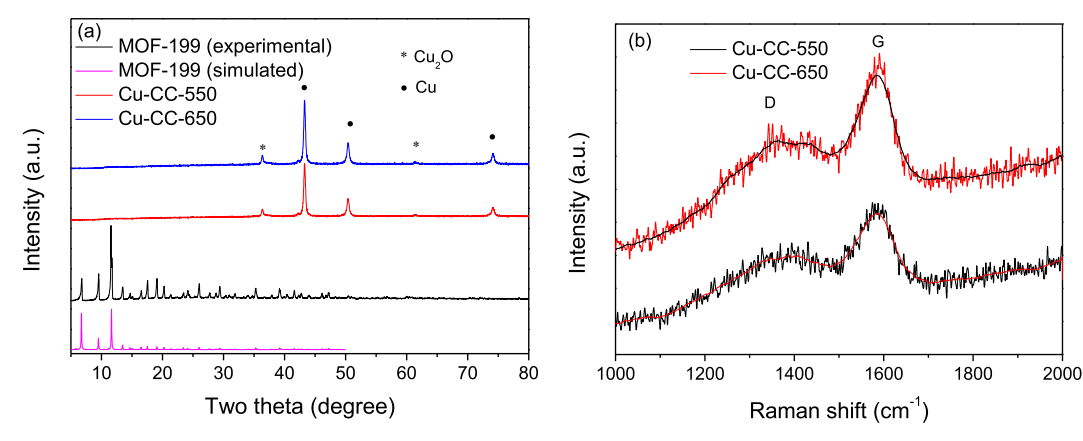
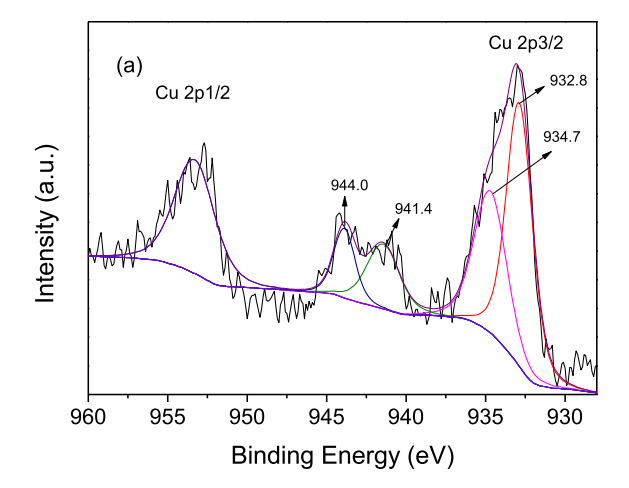
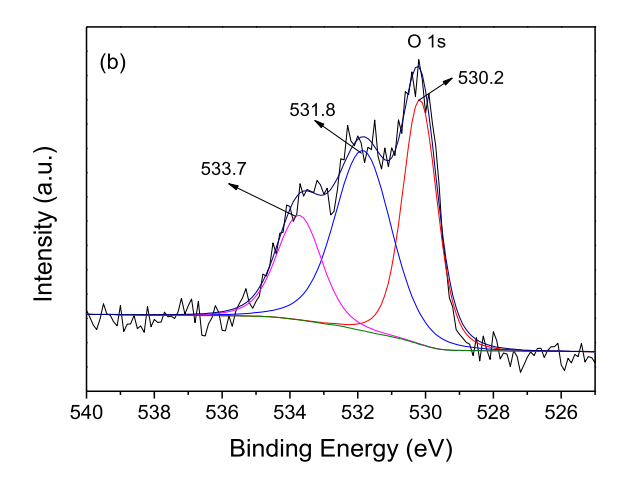


Fig. 1. (a) XRD patterns of the MOF-199 (experimental and simulated) and derived composites; (b) Raman spectra of the prepared samples.





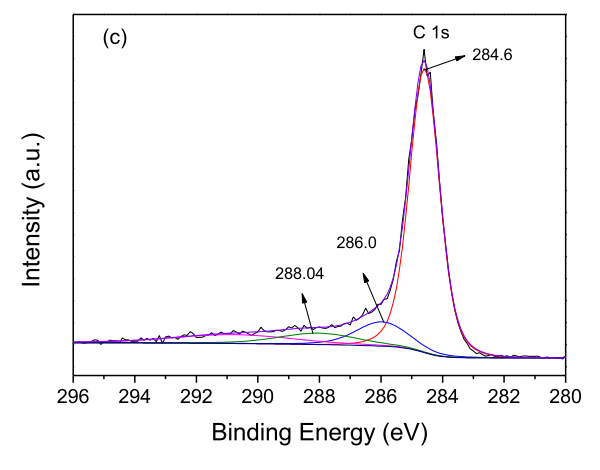


Fig. 3. High-resolution XPS spectra of (a) Cu2p, (b) O 1s, and (c) a C1s of Cu-CC-550 composite.

a small proportion of C-O (286.0 eV) and C=O (288.04 eV) phases (Fig. 3(c)) [38].

To understand the morphology, microscopic images of MOF-199 and prepared Cu-CC composites were taken using a scanning electron microscope. As observed in Fig. 4 (a), MOF-199 possesses a double-sided pyramidal shape with clear shapes and distinct edges with (111) facets having particle sizes ranging in10–20 μ m [39]. However, after calcination at 550 °C, the double-sided pyramidal shape was almost collapsed (Fig. 4(b), resulting in an irregularly

shaped morphology. Similarly, calcination at 650 $^{\circ}$ C also resulted in highly irregular and disordered surface morphology (Fig. 4(c).

3.2. Catalytic decoloration of dyes and plausible mechanisms

The catalytic decoloration of MB was investigated by monitoring the characteristic absorption peak at 664 nm ($\Lambda_{max~(MB)}$). NaBH₄ did not significantly affect the MB concentration in the absence of catalyst, only to give a slight decrease in peak intensity after 30 min reaction. The decrease of the peak intensity is likely due to the reduction of MB by NaBH₄ in the bulk phase reaction (Fig. S1). Fig. 5(a) shows the catalytic decoloration of MB by Cu-CC-550 in the presence of 0.2 M NaBH₄ solution. The addition of Cu-CC-550 to MB solution (18.51 mg L⁻¹) at a dose of 0.12 g L⁻¹ significantly reduced the absorbance, and within 270 s the bright blue solution was gradually bleached to colorless solution. Similarly, Cu-CC-650 was very effective in decoloring MB solution, showing quite comparable catalytic activity to Cu-CC-550 (Fig. S2).

The optimization of NaBH₄ concentration is an important issue as it governs the overall reaction efficiency. To determine the effect of NaBH4 concentration, a series of kinetics experiments were conducted in a way that the amounts of MB (18.51 mg L^{-1}) and Cu- $CC-550 \, (0.12 \, g \, L^{-1}))$ were kept constant while NaBH₄ concentration was varied. The time courses of MB decoloration at varying NaBH₄ concentration are shown in Fig. 5(b), and the corresponding pseudo-first-order rate constants ($k_{\rm app}$, detail is given in Supplementary materials) are presented in Table S2. The values of k_{app} were found to increase with the increase of NaBH₄ concentration up to 0.2 M. but further increase of NaBH₄did not result in kinetics increase. The increase of reaction kinetics by increment of NaBH4 up to 0.2 M could be attributable to increased availability of BH₄ that served as a reductant upon binding to the catalyst [4]. Above 0.2 M, it appears the catalytic surface became fully saturated and that no further enhancement of MB decoloration was observed. Therefore, 0.2 M NaBH₄ was considered as an optimal dose, and employed in further experiments.

For RB, the characteristic absorption peak was found at 553 nm ($\Lambda_{\rm max~(RB)}$), and similar to MB, the presence of NaBH₄ did not significantly influence RB reduction without catalyst (Fig. S3). Fig. 6 shows the result of catalytic decoloration of RB by Cu-CC-550 in the presence of 0.2 M NaBH₄. After the addition of Cu-CC-550, at a dose of 0.11 g L⁻¹, the pink colored RB solution (25.28 mg L⁻¹) rapidly bleached to colorless solution within 180 s. The rate of RB decoloration ($k_{\rm app}=0.02$) was slightly higher than that of MB ($k_{\rm app}=0.017$), which is consistent with a previous study [12].

Considering the practical aspect, it is essential to check the catalyst's activity to treat dyes in a mixture. Cu-CC-550 demonstrated high catalytic efficiency towards decoloration of the MB and RB mixture, showing complete decoloration within 480 s (Fig. 7). A comparison of the decoloration of MB and RB by some other novel or non-noble metal-based catalysts reported in the literature is presented in Table 1, and it revealed that Cu-CC-500 exhibited comparable or superior catalytic performance to other types of catalysts.

Separate experiments were conducted to confirm the role of Cu components in Cu-CC-550. Cu-CC-550 was treated with dilute HCl followed by conc. HNO₃ to dissolve all the metal/metal oxide phases, and the resulting product was thoroughly rinsed with water and ethanol, and dried. The sample was named as Cu-CC-AT (AT referred as acid treated). The XRD confirmed that all the Cu-components have been removed, leaving only carbons behind (Fig. S4). The UV-vis spectrum of MB after reaction with Cu-CC-AT in the presence of NaBH₄ is presented in Fig. 8, along with the spectrum obtained with Cu-CC-550 for a comparison. The result shows only a small decrease in absorption peaks as compared to the

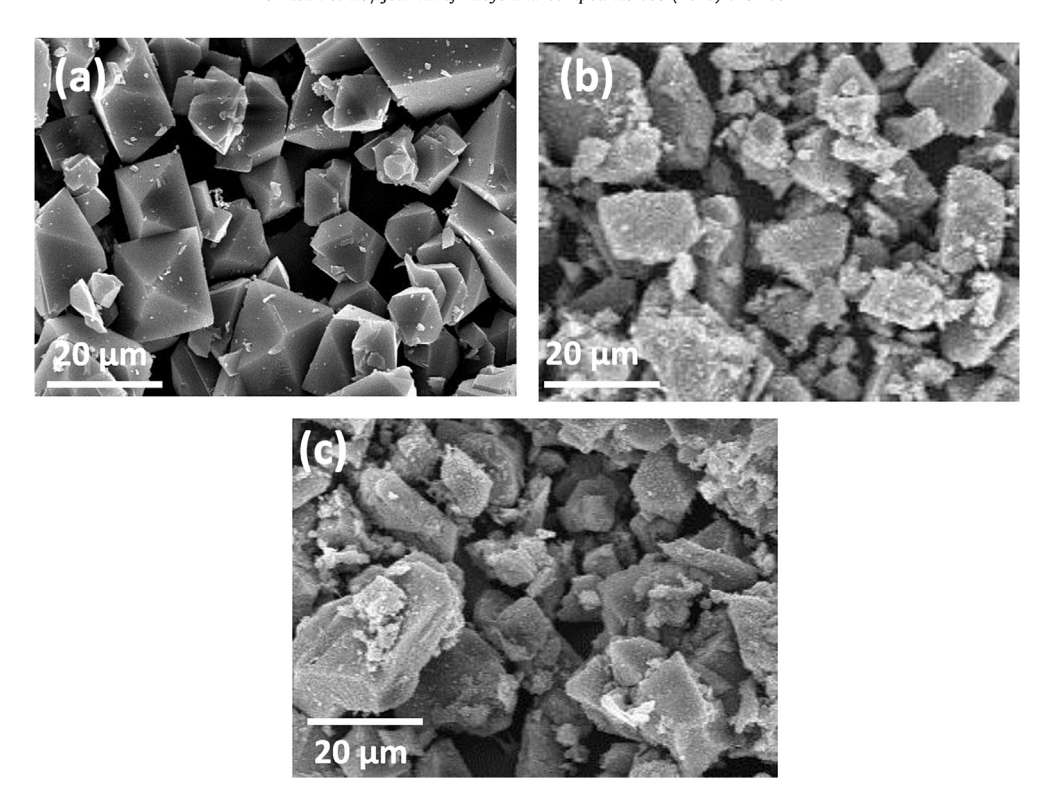


Fig. 4. Fe-SEM images of (a) MOF-199, (b) Cu-CC-550, and (c) Cu-CC-650.

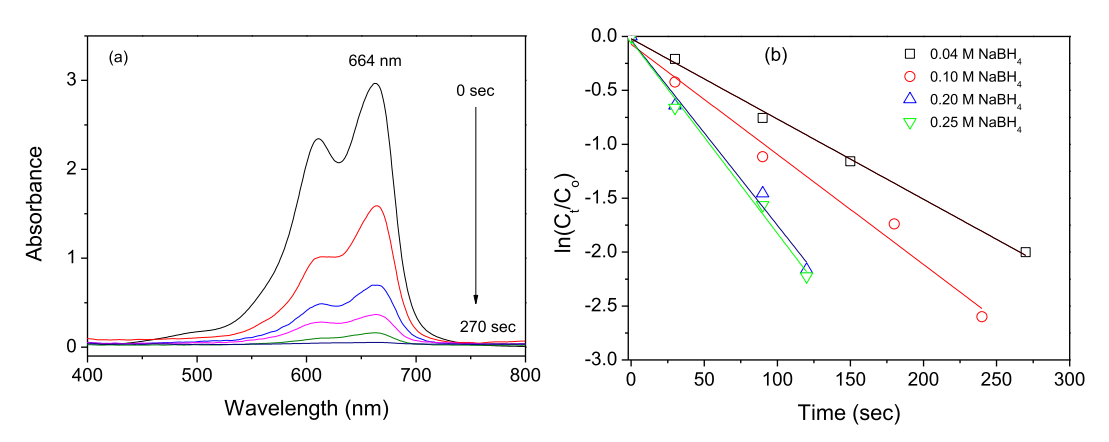


Fig. 5. (a) Time dependent UV—Vis spectral changes for the decoloration of MB solution in the presence of 0.20 M NaBH₄ by Cu-CC-550 composite; (b) Pseudo first-order kinetic plots (ln (C_t/C_o) Vs t) to check the effect of concentration of NaBH₄ on decoloration of MB by Cu-CC-550 composite.

blank sample. From this result, it is obvious that Cu plays a key role in catalytic decoloration of MB.

It has been well demonstrated that transition metals, mostly noble metals, can reduce dye chemicals in the presence of NaBH₄ [41,45–49], and many of those reductions were explained with Langmuir–Hinshelwood mechanism [47–49]. Recently, several non-novel metal catalysts (based on Cu or Co nano particles) have been reported to show good catalytic activity in reduction of dyes [21,50,51]. Besides, Gopal et al. [52] reported that first row transition metal oxides (metal having electronic configuration d^n ($n \sim 5-9$)) are also very effective in catalytic reduction of dyes, and this findings was further validated by Qiu et al. [53]who demonstrated catalytic activity of Cu₂O-boron nitride composites. Similarly in this study, the prepared composites possessed both Cu and Cu₂O phases, and showed good catalytic activity in reduction of azo dyes. The catalytic reduction is assumed to proceed via 1)

adsorption of BH $_4^-$ on the metal surface with the simultaneous production of highly active nascent hydrogen [47,54,55], and 2)the nascent hydrogen on the metal surface directly reduced dye molecules adsorbed on the metal surface [53,56], or else the nascent hydrogen reduced water molecules to produce H $_2$, which subsequently served as a reductant for dyes [47].

3.3. Reusability

Considering the economical as well as environmental aspects, reusability of a catalyst becomes an important issue. Therefore, the reusability of Cu-CC-550 was evaluated by running repetitive reduction cycles. After each run, Cu-CC-550 was separated by filtration and washed with ethanol and water for regeneration. The results of MB decoloration in five consecutive reactions are presented in Fig. 9. The catalyst exhibited considerable reusability as

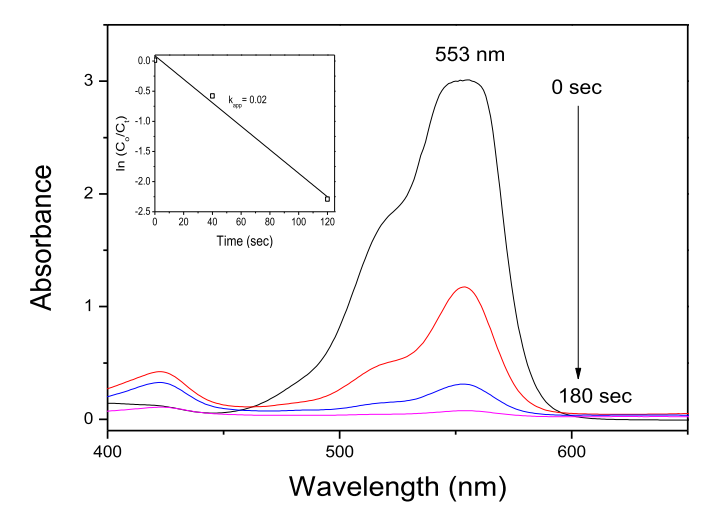


Fig. 6. Time dependent UV—Vis spectral changes for the decoloration of RB in the presence of 0.20 M NaBH_4 by Cu–CC-550 composite. Inset shows the Pseudo first-order kinetic plots ($\ln (C_t/C_o)$ Vs t).

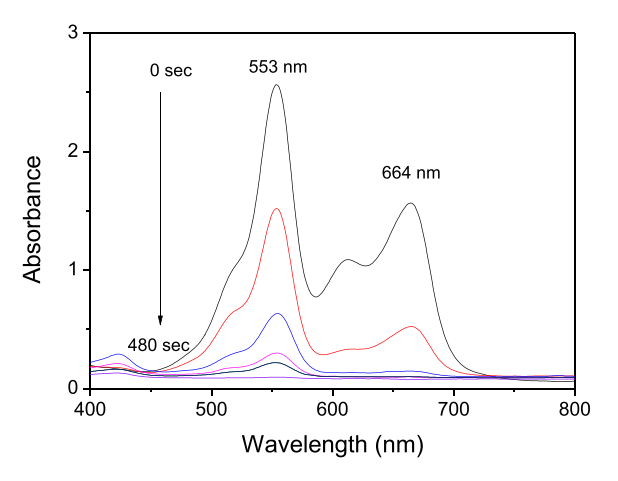


Fig. 7. Time dependent UV–Vis spectral changes for the decoloration of mixed dye (MB + RB) in the presence of 0.20 M NaBH $_4$ by Cu–CC-550 composite.

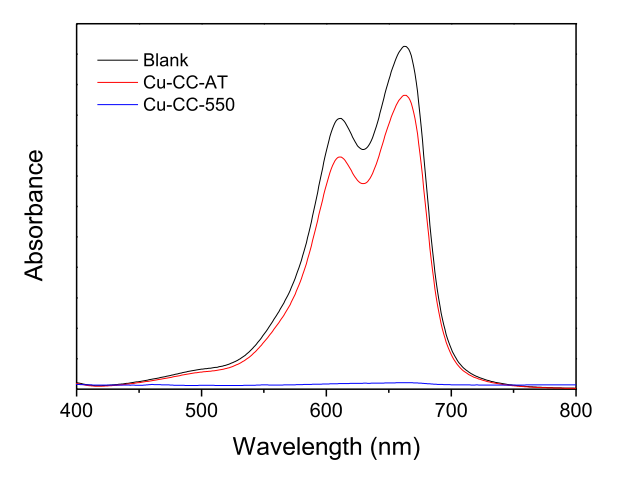


Fig. 8. Comparison of the decoloration efficiency of MB solution in the presence of 0.20~M NaBH $_4$ by Cu-CC-550 and Cu-CC-AT Composite.

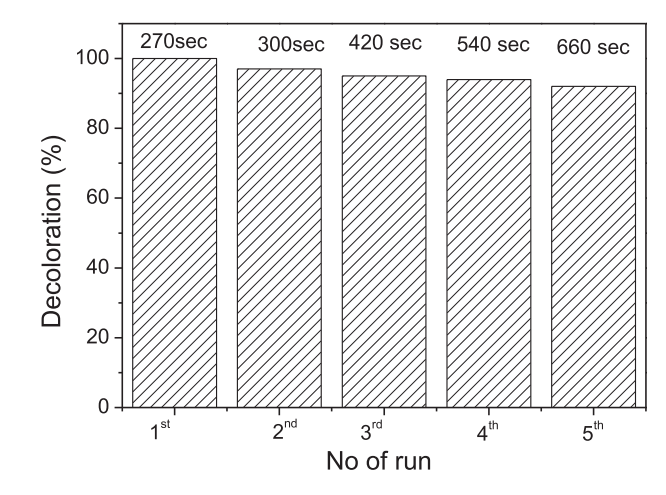


Fig. 9. Decoloration percentage of MB in five successive cycles with Cu-CC-550 catalyst and the time required to complete each cycle.

 $\begin{tabular}{ll} \textbf{Table 1} \\ \textbf{Comparison of various catalysts in the decoloration of MB and RB dyes with NaBH_4.} \\ \end{tabular}$

Catalyst	Dye	Catalyst conc. (mg/ml)	Dye conc. (mg/L)	NaBH ₄ conc.(M)	Time (sec)	Reference
Ag/TiO ₂	МВ	0.06	9.8	2.7×10^{-3}	165 s	[40]
Fe ₃ O ₄ @C@Au		0.33	3.1	5.0×10^{-3}	600 s	[41]
Gold _{core} -polyaniline _{shell}		0.05	15.9	5.0×10^{-2}	300	[14]
MnFe ₂ O ₄ @SiO ₂ @Ag		0.33	10.6	3.0×10^{-2}	660	[42]
Fe₃O₄@Nico-Ag		0.33	10.6	3.0×10^{-2}	300	[43]
Cu-CC-550		0.12	18.5	5.0×10^{-2}	270	This work
ZrO ₂ /Ag	RB	0.20	5.4	4.5×10^{-3}	480	[44]
Gold _{core} -polyaniline _{shell}		0.05	23.9	5.0×10^{-2}	360	[14]
MnFe ₂ O ₄ @SiO ₂ @Ag		0.33	15.7	3.0×10^{-2}	150	[42]
Fe₃O₄@Nico-Ag		0.33	15.7	3.0×10^{-2}	600	[43]
Cu-CC-550		0.11	25.28	5.0×10^{-2}	180	This work

more than 92% conversion was achieved after five consecutive cycles. However, the time required to complete each cycle (at least 92% conversion) gradually increased from 270 s in the first cycle to 660 s in the fifth cycle (Fig. 9), indicating a slight decrease in catalytic efficiency. This may be due to leaching of minute amounts of Cu species or partial blocking of active sites during repeated reduction experiments. Moreover, the retention of structural

integrity of the material was confirmed by XRD analysis of Cu-CC-550 recovered after the fifth cycle (Fig. S5).

4. Conclusion

In this study, highly porous non-noble metal Cu-carbon composites were prepared by heat treatment of MOF-199 under N_2

atmosphere. The inherited double-sided pyramidal morphology of MOF-199 was destroyed upon heat treatment, giving rise to the formation of Cu₂O/Cu particles dispersed on amorphous carbon network. Cu-CC-650 composite exhibited a bit higher surface area compared to Cu-CC-550 composite, however, no significant difference in the efficiencies in catalytic decoloration of MB. NaBH₄ concentration was optimized as 0.20 M. Cu-CC-550 was a very effective catalyst that it, at a dose of 0.11 g L $^{-1}$, completely decolorized MB, RB and their mixture in 270, 180, and 480 s, respectively. Moreover, Cu-CC-550 showed robust reusability to complete five consecutive reduction cycles with a small loss of catalytic capability and structural integrity. Finally, considering all these favorable features, the Cu-CC composites can be further advanced into an efficient, cost-effective and reusable catalyst for decoloration of commercial dyes.

Acknowledgment

This work was supported by Korea Research Foundation (Ministry of Education, NRF-2014R1A1A2054607).

Appendix A. Supplementary data

Supplementary data related to this article can be found at http://dx.doi.org/10.1016/j.jallcom.2016.08.027.

References

- [1] M.T. Yagub, T.K. Sen, S. Afroze, H.M. Ang, Adv. Colloid. Interface Sci. 209 (2014) 172–184.
- [2] M.T. Yagub, T.K. Sen, H.M. Ang, Water Air Soil Poll. 223 (2012) 5267-5282.
- [3] B. Mu, A. Wang, J. Environ. Chem. Eng. 4 (2016) 1274–1294.
- [4] Z. Hasan, D.-W. Cho, I.-H. Nam, C.-M. Chon, H. Song, Materials 9 (2016) 261.
- [5] M.A.M. Salleh, D.K. Mahmoud, W.A.W.A. Karim, A. Idris, Desalination 280 (2011) 1–13.
- [6] D.-W. Cho, B.-H. Jeon, C.-M. Chon, F.W. Schwartz, Y. Jeong, H. Song, J. Ind. Eng. Chem. 28 (2015) 60–66.
- [7] S.S. Moghaddam, M.R.A. Moghaddama, M. Arami, J. Hazard. Mater 175 (2010) 651–657.
- [8] H. Zou, M. Song, F. Yi, L. Bian, P. Liu, S. Zhang, J. Alloy. Compd. 680 (2016) 54–59.
- [9] E.S. Aazam, R.M. Mohamed, J. Alloy. Compd 577 (2013) 550–555.
- [10] C.Y. Teh, P.M. Budiman, K.P.Y. Shak, T.Y. Wu, Ind. Eng. Chem. Res. 55 (2016) 4363–4389.
- [11] R.S. Blackburn, Environ. Sci. Technol. 38 (2004) 4905-4909.
- [12] B.K. Ghosh, S. Hazra, B. Naik, N.N. Ghosh, Powder Technol. 269 (2015) 371–378.
- [13] S. Xuan, Y.-X.J. Wang, J.C. Yu, K.C.-F. Leung, Langmuir 25 (2009) 11835—11843.
- [14] S. Dutt, P.F. Siril, V. Sharma, S. Periasamy, New J. Chem. 39 (2015) 902–908.
- [15] X.-H. Li, X. Wang, M. Antonietti, Chem. Sci. 3 (2012) 2170–2174.
- [16] N. Yan, Z. Zhao, Y. Li, F. Wang, H. Zhong, Q. Chen, Inorg. Chem. 5 (2014) 9073–9079.
- [17] M. Ajmal, M. Siddiq, H. Al-Lohedanc, N. Sahiner, RSC Adv. 4 (2014) 59562–59570.
- [18] M. Nasrollahzadeh, M. Atarod, S.M. Sajadi, Appl. Surf. Sci. 364 (2016)

- 636-644.
- [19] M. Nasrollahzadeh, M. Atarod, B. Jaleh, M. Gandomirouzbahani, Ceram. Int. 42 (2016) 8587–8596.
- [20] L. Pan, T. Muhammada, L. Maa, Z.-F. Huang, S. Wang, L. Wang, J.-J. Zou, X. Zhang, Appl.Catal. B Environ. 189 (2016) 181–191.
- [21] Z. Hasan, D.-W. Cho, C.-M. Chon, K. Yoon, H. Song, Chem. Eng. J. 298 (2016) 183–190.
- [22] X. Li, C. Zeng, J. Jiang, L. Ai, J. Mater. Chem. A 4 (2016) 7476-7482.
- [23] K.-Y.A. Lin, S.-Y. Chen, ACS Sustain. Chem. Eng. 3 (2015) 3096–3103.
- [24] G. Férey, Chem. Soc. Rev. 37 (2008) 191–214.
- [25] S.H. Jhung, N.A. Khan, Z. Hasan, CrystEngComm 14 (2012) 7099-7109.
- [26] Z. Hasan, S.H. Jhung, J. Hazard. Mater 283 (2015) 329-339.
- [27] W. Chaikittisilp, K. Ariga, Y. Yamauchi, J. Mater. Chem. A 1 (2013) 14-19.
- [28] N.L. Torad, M. Hu, S. Ishihara, H. Sukegawa, A.A. Belik, M. Imura, K. Ariga, Y. Sakka, Y. Yamauchi, Small 10 (2014) 2096—2107.
- [29] D. Britt, D. Tranchemontagne, O.M. Yaghi, Proc. Natl. Acad. Sci. 105 (2008) 11623–11627.
- [30] J. Hu, H. Yu, W. Dai, X. Yan, X. Hua, H. Huang, RSC Adv. 4 (2014) 35124—35130.
- [31] Y. Li, Q. Wang, P. Liu, X. Yang, G. Dun, Y. Liu, Ceram. Int. 41 (2015) 4248–4253.
- [32] J. Jiang, H. Chen, Z. Wang, L. Bao, Y. Qiang, S. Guan, J. Chen, J. Colloid Interface Sci. 452 (2015) 54–61.
- [33] M.C. Biesinger, L.W.M. Lau, A.R. Gerson, R. St. C. Smart, Appl. Surf. Sci. 257 (2010) 887–898.
- [34] M. Valvo, D. Rehnlund, U. Lafont, M. Hahlin, K. Edström, L. Nyholm, J. Mater. Chem. A 2 (2014) 9574–9586.
- [35] J. Park, K. Lim, R.D. Ramsier, Y.C. Kang, Bull. Korean Chem. Soc. 32 (2011) 3395—3399.
- [36] T. Robert, M. Bartel, G. Offergeld, Surf. Sci. 33 (1972) 123-130.
- [37] M.K. Rajumon, K. Prabhakaran, C.N.R. Rao, Surf. Sci. 233 (1990) L237–L242.
- [38] J.M. González-Domínguez, P. Castell, S. Bespín-Gascón, A. Ansón-Casaos, A.M. Díez-Pascual, M.A. Gómez-Fatou, A.M. Benito, W.K. Maser, M.T. Martínez, J. Mater. Chem. 22 (2012) 21285—21297.
- [39] M. Shöaee, J.R. Agger, M.W. Anderson, M.P. Attfield, Cryst. Eng. Comm. 10 (2008) 646–648.
- [40] M. Atarod, M. Nasrollahzadeh, S.M. Sajadi, J. Colloid Interface Sci. 462 (2016) 272–279
- [41] Z. Gan, A. Zhao, M. Zhang, W. Tao, H. Guo, Q. Gao, R. Mao, E. Liu, Dalton Trans. 42 (2013) 8597–8605.
- [42] U. Kurtan, M. Amir, A. Yıldız, A. Baykal, Appl. Surf. Sci. 376 (2016) 16–25.
- [43] U. Kurtan, Md Amir, A. Baykal, Appl. Surf. Sci. 363 (2016) 66–73.
- [44] J. Ma, S. Guo, X. Guo, H. Ge, Ceram. Int. 41 (2015) 12453—12458.
- [45] M. Tajbakhsh, H. Alinezhad, M. Nasrollahzadeh, T.A. Kamali, J. Alloy. Compd. 685 (2016) 258–265.
- [46] A. Rostami-Vartooni, M. Nasrollahzadeh, M. Alizadeh, J. Alloy. Compd. 680 (2016) 309–314.
- [47] D. Xu, P. Diao, H. Baida, T. Jin, X. Guo, M. Xiang, Y. Yang, H. Li, J. Appl. Catal. A Gen. 516 (2016) 109–116.
- [48] B. Baruah, G.J. Gabriel, M.J. Akbashev, M.E. Booher, Langmuir 29 (2013) 4225–4234.
 [49] W. Stefanie, P. Frank, J. Van, M. Vu, M. Ballauff, J. Phys. Chem. C 114 (2010)
- [49] W. Stefanie, P. Frank, L. Yan, M. Yu, M. Ballauff, J. Phys. Chem. C 114 (2010) 8814—8820.
- 50] J. Feng, L. Su, Y. Ma, C. Ren, Q. Guo, X. Chen, Chem. Eng. J. 221 (2013) 16–24.
- [51] P. Zhang, Y. Sui, G. Xiao, Y. Wang, C. Wang, B. Liu, G. Zou, B. Zou, J. Mater. Chem. A 1 (2013) 1632–1638.
- [52] T.R. Mandlimath, B. Gopal, J. Mol. Catal. A Chem. 350 (2011) 9–15.
- [53] C. Huang, W. Ye, Q. Liu, X. Qiu, ACS Appl. Mater. Interfaces 6 (2014) 14469–14476.
- [54] M.C.S. Escñno, E. Gyenge, R.L. Arevalo, H. Kasai, J. Phys. Chem. C 115 (2011) 19883—19889.
- [55] D. Xu, P. Diao, T. Jin, Q. Wu, X. Liu, X. Guo, H. Gong, F. Li, M. Xiang, Y. Ronghai, ACS Appl. Mater. Interfaces 7 (2015) 16738–16749.
- [56] Y.G. Hu, T. Zhao, P.L. Zhu, X.W. Liang, R. Sun, C.P. Wong, RSC Adv. 5 (2015) 58–67.